SOLID STATE LASERS
AND NONLINEAR FREQUENCY CONVERSION

Frequency Conversion in Nonlinear Photonic Crystal of Strontium Tetraborate

A. S. Aleksandrovsky[a, b], A. M. Vyunishev[a, b], A. I. Zaitsev[a, b], A. A. Ikonnikov[b],
G. I. Pospelov[b], V. E. Rovskii[b], and V. V. Slabko[b]

[a] *Kirensky Institute of Physics, Siberian Branch, Russian Academy of Sciences, Krasnoyarsk, 660036 Russia*
[b] *Siberian Federal University, Krasnoyarsk, 660041 Russia*
e-mail: aleksandrovsky@kirensky.ru
Received January 20, 2011

Abstract—Using a nonlinear photonic crystal (NPC) of strontium tetraborate, we obtained the second-harmonic generation of femtosecond pulses in the nonlinear diffraction regime with an efficiency of 1.9% that is tunable in the near-UV spectral range, as well as fourth-harmonic generation under the conditions of random quasi-phase-matching with maximum efficiency of 10^{-5} that is tunable in the far-UV spectral range. The efficiency of second-harmonic generation in strontium tetraborate NPC under the conditions of random quasi-phase-matching was significantly lower. The fourth-harmonic was tunable between 187.5 and 232.5 nm. The previously predicted red shift of spectral components in the generated radiation spectrum upon NPC rotation is demonstrated experimentally.

INTRODUCTION

The invention of lasers 50 yeas ago stimulated the development of nonlinear optics. Currently, methods of nonlinear optics are widely used for the frequency conversion of radiation to different spectral ranges, thus complementing methods of laser generation. The efficiency of nonlinear-optical interaction critically depends on the parameters of used homogeneous nonlinear media. The mechanisms of the frequency conversion in these media are well studied. Today, the attention of specialists working in the area of nonlinear optics is focused on studying the properties of spatially inhomogeneous nonlinear media [1]. These media represent a sequence of areas with periodically changing orientation of the static polarization vector and sign of the second-order nonlinear susceptibility, which enables the partial compensation for the phase mismatch between the interacting waves in the process of nonlinear-optical conversion, thus leading to efficient generation in cases where angular phase-matching is unavailable. An extreme case of this medium is a regular domain structure (RDS) wherein both the quasi-phase-matching [2] and the nonlinear diffraction [3] regimes are realized. In general, regular, as well as irregular, domain structures can be considered as nonlinear photonic crystals (NPC) [4]. Nonlinear-optical frequency conversion becomes possible in irregular structures both due to random quasi-phase-matching [5] and nonlinear diffraction [6, 7]. The advantages of the aforementioned types of phase matching are the possibility of using maximal tensor components of the nonlinear susceptibility of the

medium that are usually inaccessible under angular phase-matching (the restrictions on the polarization of the interacting waves are lifted out), the fact that angular and spectral characteristics are not critical, and the possibility of conversion of all spectral components with equal efficiency [7], which is important in the case of frequency conversion of ultrashort light pulses. Domain structures in ferroelectric crystals, such as KDP, KTP, $LiNbO_3$, $LiTaO_3$, strontium barium niobate (SBN), and other crystals belong to this type of media.

Despite the achievements of modern nonlinear optics, the far-UV spectral range remains essentially unexplored. In particular, angular phase matching for second-harmonic generation (SHG) is possible to achieve only down to 205 nm in BBO. Further advancement into a shorter wavelength range of the spectrum is possible via sum-frequency generation, which in turn leads to the significant complication of the experimental setup. To this end, typically, high-power femtosecond laser systems that include regenerative amplifiers and contain a large number of nonlinear crystals are used, which implies the use of delay stages for pulse synchronization. A detailed analysis of the generation of radiation in the wavelength range near 200 nm via angular phase-matching has been given in [8]. The situation is further complicated by the limited choice of ferroelectric crystals transparent in the far-UV spectral range. Only one known ferroelectric crystal, $MgBaF_4$, has a transparency range that enables the generation of radiation down to 140 nm [9]. This crystal, however, is not widely used
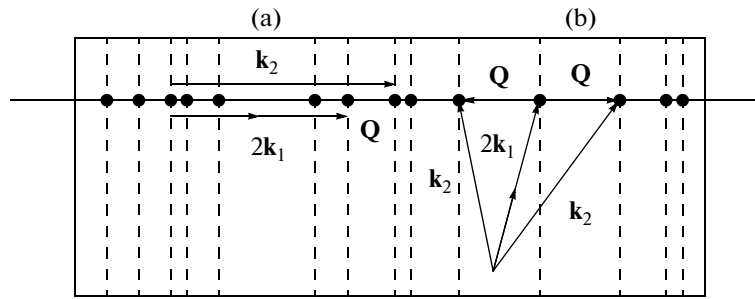
Fig. 1. Phase-matching diagram in reciprocal space: (a) random quasi-phase-matching, (b) nonlinear diffraction.

because its nonlinear coefficients are extremely small. In contrast, strontium tetraborate has the highest non-linearities among the crystals transparent in the far-UV spectral range, and its transparency range extends down to 125 nm [10]. Although this crystal lacks angular phase matching for SHG [11], previous studies underscored an unusual dependence of the second-harmonic signal on the propagation angle inside the crystal [12] and a high conversion efficiency of up to 1% [11, 12], which is not typical for non-phase-matched generation. Previously, we have established that strontium tetraborate crystal has a tendency to form irregular domain structures [13]; thus, it can be considered as an NPC.

Here, we report the results of experimental studies of frequency conversion of radiation in an NPC of strontium tetraborate (SBO) to near- and far-UV spectral ranges. There are two limiting geometries of phase matching, which are determined by the relative position of pump and reciprocal lattice vectors of NPC, which are shown in Fig. 1. In the case where these vectors are parallel, only a random quasi-phase-matching takes place [14]; otherwise, both random quasi-phase-matching and nonlinear diffraction are possible [15]. In vector form, the phase-matching condition for these two cases is given by

$$\mathbf{k}_2 = 2\mathbf{k}_1 \pm \mathbf{Q}, \qquad (1)$$

where $\mathbf{k}_{1,2}$ are the wave vectors of the pump and the second harmonic waves, respectively; $\mathbf{Q} = \pi m/d$ is the reciprocal lattice vector that has a continuum of allowed values in an irregular NPC; d is the thickness of an individual domain; and $m = \pm 1, \pm 3, \ldots$ is the quasi-phase-matching order. Depending on the domain distribution, a particular structure can favor either nonlinear diffraction or random quasi-phase-matching in a given spectral range because different reciprocal-lattice wave vectors are involved in these processes. However, in the case of an irregular domain structure, the possibility of generating tunable radiation in a wide spectral range is common for both processes.

EXPERIMENTAL RESULTS; NONLINEAR DIFFRACTION

The effect of nonlinear diffraction can be observed upon the propagation of pump radiation parallel to the crystallographic *b* axis. The studied SBO sample No. 1 that contained irregular domain structures was $6 \times 6.5 \times 5$ mm in size. A Tsunami femtosecond laser (Spectra-Physics) tunable at 710−1020 nm was used as a pump source. The laser pulse width was 40−100 fs. The laser radiation with an average power of up to 1 W was focused into the crystal by a lens with a 10-cm focal distance. The polarization of the pump radiation was parallel to the crystallographic *c* axis of the crystal. Under the normal incidence of the pump radiation on the input face of the crystal, two highly directed beams of the second harmonic that were deviated by equal angles to both sides of the pump beam were observed (Fig. 2). For the normal incidence of the fundamental radiation with the central wavelength of 800 nm, the nonlinear diffraction angle measured from the direction of propagation of the pump radiation was 16.6°. This value is in good agreement with the value of 16.9° calculated from the phase-matching diagram (Fig. 1).
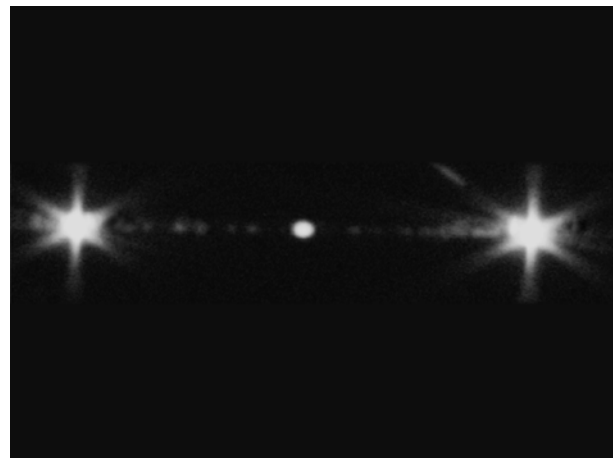

Fig. 2. Nonlinear diffraction in strontium tetraborate NPC. Central spot corresponds to a non-phase-matched SHG.
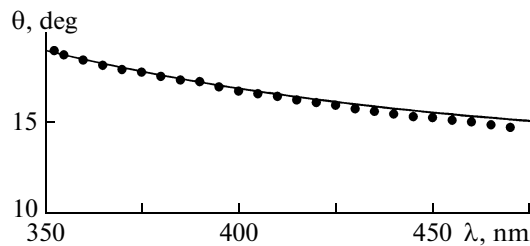
Fig. 3. Spectral dependence of nonlinear-diffraction angle.

Fig. 4. Spectra of pump radiation (*1*) and second harmonic (*2*).

Figure 3 shows the calculated and experimental dependences of the nonlinear-diffraction angle on the central wavelength of the second-harmonic radiation. A small difference between the calculated and the experimental values in the long-wavelength range can be attributed to limited precision with which the coefficients in the Sellmeier equation, which governs the SBO index of refraction are known [11].

The spectra of pump and second-harmonic radiation were recorded with Ocean Optics USB4000 and HR4000 spectrometers, respectively. Figure 4 shows the spectra of the pump radiation (with the central wavelength of 800 nm) and the second harmonic. The average pump power was 840 mW. The spectrum of the pump radiation did not reveal any indication of self-phase modulation and caused by it broadening observed in SBN crystal [7]. For various wavelengths, the second-harmonic spectrum shows a narrowing of about 10−20% on the frequency scale as compared to the pump-radiation spectrum. A relatively smooth spectrum of the second harmonic is explained by a lower energy resolution of the HR4000 spectrometer in the short-wavelength range.

Continuum of reciprocal-lattice vectors, which is typical of irregular domain structures allows generation of radiation tunable in a wide spectral range. Figure 5a shows the spectral dependence of the average power of the second harmonic for the case where the crystal position relative to the pump beam was fixed (curve *1*) and for the case where NPC was tuned to a maximal power of the second harmonic at a given pump wavelength (curve *2*). The tuning was accomplished by translating the crystal parallel to the crystallographic *a* axis and by rotating about the crystallographic *c* axis, so that different parts of the domain structure the spectrum of the reciprocal-lattice vectors of which was the most favorable for efficient conversion were exposed to the pump radiation. The spectral range where an efficient SHG was obtained extends from 510 to 355 nm. The maximal average power of the generated radiation at the second-harmonic frequency was 5.6 mW in a single beam when pumped by radiation with the central wavelength of 800 nm and average power of 0.98 W. The conversion efficiency to second harmonic was 0.57%. Spectral dependence of
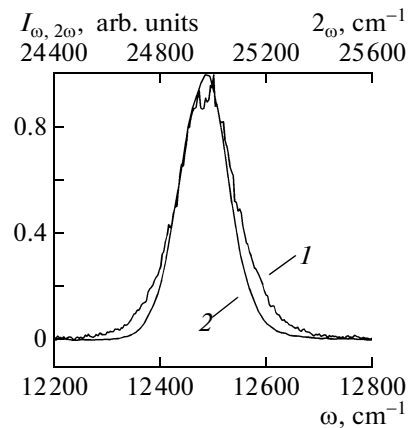
the average second-harmonic power contains a contribution from the tuning curve of the pump laser; however, single maxima and minima reflect the spectrum of reciprocal lattice vectors of the NPC. This spectrum can be revealed by getting rid of the energy parameters via normalization of the second-harmonic power to pump power squared (Fig. 5b). The obtained dependence shows that the spectrum of effective reciprocal-lattice vectors involved in the nonlinear-optical frequency conversion is sufficiently broad, but, simultaneously, contains maxima and minima.

When using a 5-cm lens, the maximal average power of the second harmonic with the central wavelength of 400 nm was 17.4 mW in two beams for a
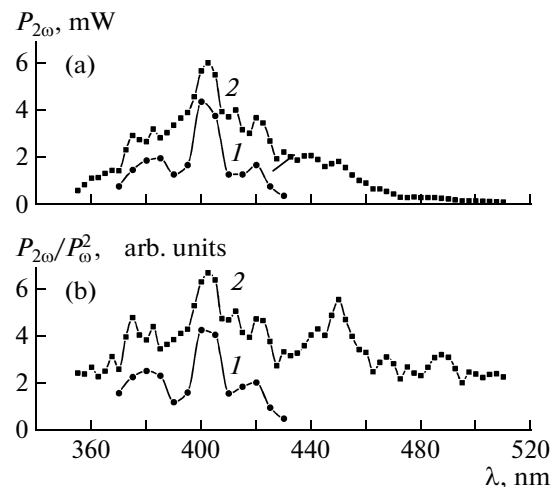

Fig. 5. (a) Spectral dependence of the average power of second harmonic of the femtosecond laser in a single beam. (b) Obtained spectrum of reciprocal-lattice vectors of the NPC. (*1*) For fixed NPC position, (*2*) with NPC tuning.
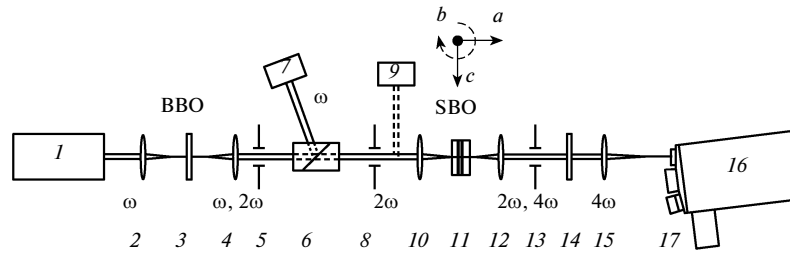
Fig. 6. Experimental arrangement for FHG: (*1*) Ti-sapphire laser; (*2, 4*) 10-cm lens; (*3*) BBO crystal; (*5, 8, 13*) iris diaphragm; (*6*) Glan prism; (*7*) pump-radiation beam block; (*9*) SHG power meter; (*10, 12*) 5-cm lens; (*11*) SBO NPC; (*14*) interference filter; (*15*) lens with a focal distance of 112 mm; (*16*) MSDD1000 monochromator; (*17*) power meter or photomultiplier.

pump power of 0.92 W. The conversion efficiency to the second harmonic was thus 1.9%, which is a factor of five higher than that obtained in [7] in an SBN crystal whose nonlinear susceptibility is a factor of 3.4 higher than that of SBO. The above efficiency sets a record among all experiments conducted so far in the nonlinear diffraction geometry. In some cases, the non-collinear scheme is preferable because it automatically separates the interacting beams in space.

RANDOM QUASI-PHASE-MATCHING

An SBO sample No. 2 with the dimensions of $5 \times 11 \times 9$ mm was used for the frequency conversion of radiation to the far-UV spectral range. The sample geometry was optimized for the frequency conversion under the conditions of random quasi-phase-matching. Preliminary results of these studies were published in [16].

First, we tested SBO sample No. 2 for SHG in the regime of nonlinear diffraction, as well as under the conditions of random quasi-phase-matching. As it turned out, sample No. 2 had lower SHG efficiency in the regime of nonlinear diffraction than sample No. 1. At the same time, the SHG efficiency under the conditions of random quasi-phase-matching was at least an order of magnitude lower than that in the regime of nonlinear diffraction. This allowed us to suggest that the nonlinear-diffraction regime is favorable in this sample from the point of view of the frequency conversion of ultrashort pulses to the far-UV spectral range.

The conducted experiments on the fourth-harmonic generation (FHG) revealed an opposite situation, that is, no signal at the fourth-harmonic frequency was detected in the nonlinear-diffraction regime. At the same time, the signal could be reliably detected in the random quasi-phase-matching geometry.

The experimental arrangement for FHG from the femtosecond laser in the random quasi-phase-matching geometry is shown in Fig. 6. The second-harmonic radiation was generated in a 1-mm thick BBO crystal cut for Type I phase-matching. The crystal was installed between two 10-cm lenses in the focal plane

of the system. The maximal average second-harmonic power reached 135 mW, which corresponds to the conversion efficiency of 14.4%. The second-harmonic radiation selected by a Glan polarizer was focused into the NPC with a 5-cm lens. The domain structure of the NPC was studied with a Carl Zeiss Axio Observer.A1m optical microscope. The structure contained 262 domains with the total length of 2.1 mm along the crystallographic *a* axis. The domain thickness varied randomly between several tenths of a micron to tens of microns. Despite the limitation on the resolution of optical microscopy imposed by the wavelength, we were able to reliably identify domains of opposite polarity by the character of etching down to 0.2-μm thickness. The measured waist radius of the second-harmonic beam was 37 μm at $1/e^2$ power level, which corresponds to the peak power of 0.3 GW/cm^2. The second-harmonic polarization was parallel to the crystallographic *c* axis, which allowed us to use the maximal nonlinear coefficient d_{ccc}. The generated radiation at the fourth-harmonic frequency was focused on the input slit of an MSDD 1000 monochromator equipped with a Hamamatsu HLS192 detector to register the spectra. The spectral sensitivity range of the matrix photodetector was 200—1100 nm. The spectral resolution of the monochromator in the spectral range under consideration was 0.023 nm (5 cm^{-1}). Either a Newport 918D detector with a Newport 1931-C power meter, or a Hamamatsu H5783-04 photomultiplier was installed at the axial output of the monochromator. An Acton 172-N interference filter with a maximal transmission at 173.5 nm was installed in front of the monochromator for suppression of the second-harmonic radiation. The maximal average power of the fourth harmonic at the central wavelength of 200 nm was 1 μW, which corresponds to the conversion efficiency of 10^{-5}.

Figure 7 shows spectra of the second and fourth harmonics. The fourth-harmonic spectrum corresponds to the case of normal incidence of the second-harmonic radiation on the NPC. Apparently, its shape is not typical for the spectrum of radiation generated under angular phase-matching conditions. While the second-harmonic spectrum is smooth, the spectrum
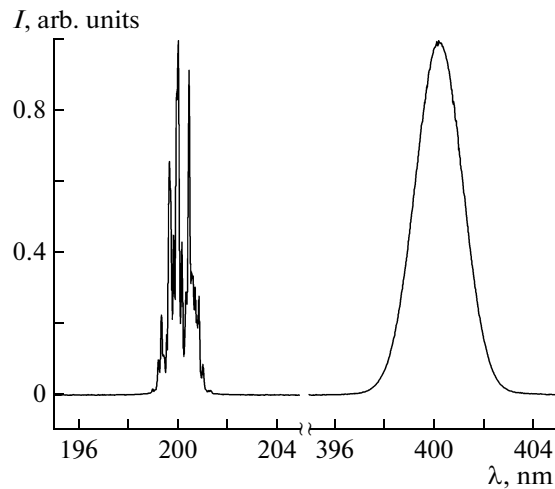
Fig. 7. Spectra of second (right) and fourth (left) harmonics of the Ti-sapphire laser.

Fig. 8. Shift of components in spectrum of generated radiation upon NPC rotation: (a) (*1*) $\lambda = 199$ nm, $\theta = 0°$; (*2*) $\lambda = 200$ nm, $\theta = 20°$; (b) (*1*) $\lambda = 199.5$ nm, $\theta = 0°$; (*2*) $\lambda = 200$ nm, $\theta = 13°$.

of the fourth harmonic consists of a series of peaks. Typically, the width of the spectral peaks was 0.1 nm, while the spacing between them varies between 0.1 and 0.3 nm. Taking into account this character of the spectrum, a distortion of temporal structure of the generated pulses is expected.

Theoretical calculations reported in [17] revealed that the destructive interference of fields generated in individual domains in irregular domain structures could be changed to a more constructive interference by rotating the NPC. An in-depth analysis [14] showed that the conversion efficiency is preserved upon simultaneous increase of the incident pump radiation wavelength and propagation angle of radiation in NPC. That is, for a pump radiation with a finite spectral bandwidth, spectral components of generated radiation will experience a shift towards longer wavelengths when the rotation angle of the NPC is increased. To test this prediction, we recorded the spectra of the generated radiation in some cases. In the first case, for the normal incidence of the second-harmonic radiation on NPC, the central wavelength of the pump radiation was varied in the vicinity of 800 nm with 1-nm steps. In the second case, the pump wavelength was kept at 800 nm, but the NPC rotation angle was varied. The results are presented in Fig. 8. Rotation of NPC or tuning the central wavelength of the pump radiation changes the spectrum of the generated radiation. At the same time, the spectra of the generated radiation maintain strict correspondence to each other depending on the central wavelength of the pump radiation and the NPC angle of rotation. At normal incidence, the shape of the spectrum centered at 199 nm is identical to that corresponding to 200 nm and the NPC angle of rotation of 20° (Fig. 8a). This effect can be explained by the compensation for the phase mismatch between the interacting waves that
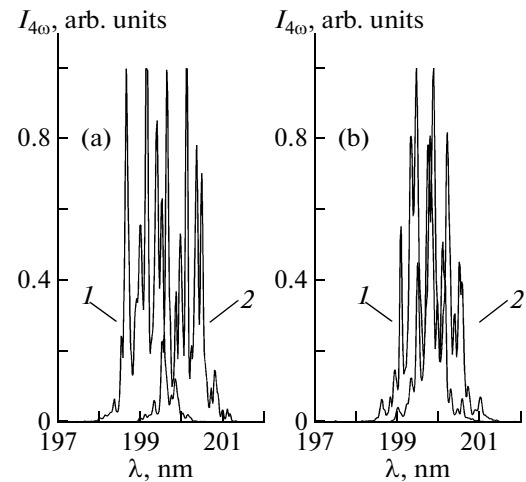
appears upon an increase in the pump wavelength as a result of the corresponding increase in optical thickness of the domains upon rotation of the NPC.

It is helpful to introduce enhancement factor in the conversion efficiency due to random quasi-phase-matching as the ratio of conversion efficiencies in an NPC and a monodomain sample. In the case of the frequency conversion of broadband radiation in an irregular NPC, the value of this factor can vary significantly within the spectral bandwidth of the generated radiation. In this case, it is convenient to define this factor in terms of spectrum-integrated power of the radiation generated in the NPC and in the reference sample. As a reference, we used a monodomain sample that had the thickness of 432 μm in the direction of the crystallographic *a* axis and was oriented such that its crystallographic *c* axis was parallel to the second-harmonic polarization. The measured factor of increase of the conversion efficiency due to random quasi-phase-matching was 320. By varying the central wavelength of the fundamental radiation, we obtained FHG from a femtosecond Ti-sapphire laser tunable in the range of 232.5–187.5 nm.

DISCUSSION

The negative result obtained in the experiment on the fourth-harmonic generation in sample No. 2 in the regime of nonlinear diffraction can be explained as follows. First, as can be seen from the table, efficient generation of radiation in this regime in the spectral range under consideration requires values of reciprocal-lattice vectors which correspond to effective domain thickness of several hundred nanometers, whereas an average domain size in sample No. 2 was 8 μm. On the contrary, in the case of the generation of radiation in the random quasi-phase-matching

Calculated values of required reciprocal-grating vectors and effective domain thickness for various nonlinear-optical processes that correspond to them

Wavelength of generated radiation, nm	Random quasi-phase-matching		Nonlinear diffraction	
	Q, μm^{-1}	$d = \pi/Q$, μm	Q, μm^{-1}	$d = \pi/Q$, μm
355−510	0.23−0.52	6.04−13.77	3.12−5.67	0.55−1.01
400	0.38	8.26	4.56	0.69
177.5−232.5	1.95−5.32	0.59−1.61	13.71−26.30	0.12−0.23
200	3.35	0.94	19.50	0.16

regime, the domain size must be several times larger than in the nonlinear diffraction regime. Second, the increase in the nonlinear diffraction angle with a decrease in the wavelength (Fig. 3) leads to the limitation of the conversion efficiency due to the limitation of the spatial overlap volume of interacting waves inside the NPC. In the case of the normal incidence of the pump radiation with the central wavelength of 400 nm, the calculated angle of propagation of the second harmonic inside the NPC is 19.5°.

Denoting the NPC contribution to the conversion efficiency due to nonlinear diffraction as F, the intensity of the generated radiation in the NPC under consideration can be expressed as

$$I_{2\omega} = \left|\chi^{(2)}\right|^2 I_\omega^2 F \big/ \left(n_1^2 n_2 S\right),$$

where $\chi^{(2)}$ is the second-order nonlinear susceptibility, and S is the beam cross-section area in the focal spot at e^{-2} level of intensity. Neglecting the difference between pulse durations of the generated radiation in the NPC under consideration, the parameter $\Re$ defined as the ratio of contributions of the NPC structure can be written as

$$\Re = \frac{F_{SBO}}{F_{SBN}} = \underbrace{\left(\frac{n_1^2 n_2 S\eta}{\left|\chi^{(2)}\right|^2 I_\omega}\right)}_{SBO} \underbrace{\left(\frac{\left|\chi^{(2)}\right|^2 I_\omega}{n_1^2 n_2 S\eta}\right)}_{SBN}, \qquad (2)$$

where η is the maximal conversion efficiency in the NPC. When the beam is focused with a 10-cm lens, the comparison using expression (2) of the NPC based on strontium tetraborate with the strontium-barium-niobate NPC used in [7] yields the value of $\Re$ equal to 46.

Considering the narrowing of the second-harmonic spectrum and the group velocity dispersion, one can suggest that the second-harmonic pulse width should be larger than that of the pump pulses. Using the expression given in [18] for the case of collinear conversion, the second-harmonic pulse width for the sample under study is estimated to be about 2 ps. However, the linear dependence of the pulse width on the length of the medium means that, for a 1-mm thick crystal, the second-harmonic pulse width would be about 350 fs. The crystal thickness must be determined based on the compromise between getting short pulses and achieving high output power of the second harmonic.

In the experiment on the frequency conversion to the far-UV spectral range, the factor of increasing the conversion efficiency due to random quasi-phase-matching was 320, in agreement with the calculated value within an order of magnitude. However, the calculated value is 800 times smaller than the value corresponding to the first-order quasi-phase-matching in RDS of the same thickness as the NPC under consideration. The significant reduction of the conversion efficiency in the NPC is the price that one has to pay to achieve generation of radiation tunable in a wide spectral range. Taking into account that the power density of the second-harmonic radiation used in our experiments was significantly lower than the optical breakdown threshold for nanosecond pulses, it is expected that the conversion efficiency can be increased considerably by using a more powerful pump source.

The main factors that determine the short-wavelength cutoff of the fourth-harmonic tuning range are absorption in air and the tuning curve of the pump laser, whereas absorption in strontium tetraborate is less of a concern. We found a peak in the absorption spectrum of the NPC material at 209 nm corresponding to absorption coefficient of 0.6 cm^{-1}. According to [10], absorption in this area is not caused by the main components of the NPC material. Presumably, involuntary admixtures cause these specific features of the absorption spectrum. Hence, with an improvement in the quality of the used materials and implementation of technologies protecting the melt from impurities during the growth process, these admixtures can be removed.

CONCLUSIONS

We have demonstrated SHG in a strontium tetraborate NPC in the nonlinear diffraction regime in the near-UV spectral range with maximum conversion efficiency of 1.9%. It was established that the contribution of NPC based on strontium tetraborate significantly exceeds that of an NPC based on strontium-

barium-niobate. The efficiency of SHG under the conditions of random quasi-phase-matching in the strontium tetraborate NPC was considerably lower. On the contrary, upon generation of radiation in the far-UV spectral range, an opposite situation took place. The fourth-harmonic signal was detected only in the random quasi-phase-matching scheme. This circumstance can be explained by the presence of the corresponding components in the spectrum of reciprocal-lattice vectors of the NPC. Due to random quasi-phase-matching, FHG from a femtosecond laser tunable from 187.5 to 232.5 nm was realized. The maximal average power of the radiation at 200 nm was 1 μW, which corresponds to the conversion efficiency of 10^{-5}. Additionally, we experimentally demonstrated the previously predicted red shift of components in the spectrum of generated radiation upon the rotation of the NPC.

REFERENCES

1. A. Arie and N. Voloch, Las. Photon. Rev. **4**, 355 (2010).
2. M. M. Fejer, G. A. Magel, D. H. Jundt, and R. L. Byer, J. Quant. Electron. **28**, 2631 (1992).
3. I. V. Shutov, I. A. Ozheredov, A. V. Shumitskii, and A. S. Chirkin, Opt. Spektrosk. **108** (1), 89 (2008).
4. V. Berger, Phys. Rev. Lett. **81**, 4136 (1998).
5. M. Baudrier-Raybaut, R. Haidar, Ph. Kupecek, Ph. Zemasson, and E. Rosencher, Nature **432**, 374 (2004).
6. I. Freund, Phys. Rev. Lett. **21**, 1404 (1968).
7. R. Fischer, S. M. Saltiel, D. N. Neshev, W. Krolikowski, and Yu. S. Kivshar, Appl. Phys. Lett. **89**, 191105 (2006).
8. V. Petrov, F. Rotermund, F. Noack, J. Ringling, O. Kittelmann, and R. Komatsu, IEEE J. Sel. Top. Quant. Electron. **5**, 1532 (1999).
9. S. C. Buchter, T. Y. Fan, V. Liberman, J. J. Zayhowski, M. Rothschild, E. J. Mason, A. Cassanho, H. P. Jenssen, and J. H. Burnett, Opt. Lett. **26**, 1693 (2001).
10. V. Petrov, F. Noack, Dezhong, Feng, Guangqui, Xiaoqing, R. Komatsu, and V. Alex, Opt. Lett. **29**, 373 (2004).
11. Yu. S. Oseledchik, A. I. Prosvirnin, V. V. Starshenko, V. Osadchuk, A. I. Pisarevsky, S. P. Belokrys, A. S. Korol, N. V. Svitanko, S. A. Krikunov, and A. F. Selevich, Opt. Mat. **4**, 669 (1995).
12. F. Pan, G. Shen, R. Wang, X. Wang, and D. Shen, J. Cryst. Growth **241**, 108 (2002).
13. A. I. Zaitsev, A. S. Aleksandrovsky, A. D. Vasiliev, and A. V. Zamkov, J. Cryst. Growth **310**, 1 (2008).
14. A. S. Aleksandrovsky, A. M. Vyunishev, I. E. Shakhura, A. I. Zaitsev, and A. V. Zamkov, Phys. Rev. A **78**, 031802 (2008).
15. A. S. Aleksandrovsky, A. M. Vyunishev, A. I. Zaitsev, A. V. Zamkov, and V. G. Arkhipkin, J. Opt. A **9**, 334 (2007).
16. A. S. Aleksandrovsky, A. M. Vyunishev, A. I. Zaitsev, and V. V. Slabko, Phys. Rev. A **82**, 055806 (2010).
17. A. S. Aleksandrovskii, A. M. V'yunyshev, I. E. Shakhura, A. I. Zaitsev, and A. V. Zamkov, Opt. Spektrosk. **107** (3), 384 (2009) [Opt. Spectrosc. **107** (3), 359 (2009)]
18. S. A. Akhmanov, V. A. Vysloukh, and A. S. Chirkin, *Optics of Femtosecond Laser Pulses* (Nauka, Moscow, 1988) [in Russian].